Pre-Print Submitted to Mechanical Research Communications

A fast iterative inverse method for turbomachinery blade design

J.C. Páscoa [a,*], A.C. Mendes [a], L.M.C. Gato [b]

[a] *Department of Electromechanical Engineering, University of Beira Interior, R. Mqs D'Avila e Bolama, 6201-001 Covilhã, Portugal*
[b] *IDMEC, Instituto Superior Técnico, Technical University of Lisbon, Av. Rovisco Pais 1, Lisboa 1049-001, Portugal*

A B S T R A C T

An improved formulation for an iterative inverse design method is presented. The method solves the time dependent Euler equations in a numerical domain where the blade sections are iteratively modified, until a prescribed blade load distribution is reached. The mean tangential velocity and thickness distributions are imposed as design variables. Each design iteration starts with a blade section modification that is impressed on the camber line. After generating a new mesh, the flow-field is updated by performing one finite volume time iteration. The blade modifications and the time-marching computation converge simultaneously to the required geometry and to the steady state flow solution. The present time-lagged formulation introduces a new blade thickness distribution term that improves the convergence rate. An empirical study on the existence and uniqueness problem is presented for the iterative inverse design method. Results for different blade cascade geometries showed the improvement of the convergence rate and the robustness of the method, for the imposed set of design conditions.

1. Introduction

The first generation of inverse methods was only capable of solving the potential flow equations. They were limited to shock-free irrotational flows and/or were difficult to extend to three-dimensions (Lighthill, 1945; Hawthorne et al., 1984). Several authors proposed iterative methods in which a geometry modification algorithm, based on the potential flow equations, is combined with an Euler or Navier–Stokes flow solver. Demeulenaere and van den Braembussche (1998) reported some problems in defining a target pressure distribution, facing thus the problem of existence and uniqueness of solution. These problems were also related to mechanical constraints, particularly regarding the blade thickness distribution.

In order to circumvent some of the limitations highlighted above, in the present approach the mean tangential velocity (that is related to the aerodynamic load) and the blade thickness distributions (Páscoa et al., 2004) are prescribed as design variables. The specification of the blade load distribution instead of the velocity, or the pressure, on both surfaces gives the user more control to avoid the occurrence of ill-posed problems. A main drawback of the method is the need to perform a dozen of analysis cycles until reaching convergence. In this work, a new formulation for the blade camber generator is presented that seeks to reduce the number of design iterations.

Inverse methods require the user to have some design experience and appreciate the subtlety of aerodynamic design in order to specify a pressure distribution for which a geometry does exists. Lighthill (1945) demonstrated that a unique and correct solution to the inverse problem does not exist unless the prescribed pressure distribution satisfies certain integral constraints. Two of those constraints arise from the requirement that the airfoil profile has a specific trailing edge thickness. A third, and subtler, constraint requires that the prescribed surface velocity distribution be compatible with the specified

* Corresponding author. Tel.: +351 275329763; fax: +351 275329972.
E-mail addresses: pascoa@ubi.pt (J.C. Páscoa), acmendes@ubi.pt (A.C. Mendes), luis.gato@ist.utl.pt (L.M.C. Gato).

free-stream velocity. Volpe and Melnik (1981) showed empirically that constraints similar to those for incompressible flow also exist for compressible flow. More recently, Daripa (1991) presented an analysis for the inverse problem in compressible flow, but the transonic problem with shock waves remains analytically unsolved (Demeulenaere and van den Braembussche, 1998; Lee and Mason, 2000).

The present work addresses two main issues. First, the development of a novel formulation that includes the thickness distribution on the blade camber generator and, second, to empirically investigate the existence and uniqueness problem for the proposed iterative inverse design method.

2. New time-lagged blade design method

The design procedure comprises two main components: the analysis code (coupled to an automatic mesh generator) and the blade modification algorithm (camber line generator).

2.1. Analysis code

In the absence of external forces and heat conduction, the two-dimensional inviscid flow, in an infinitesimal element, fixed in space, can be described by the system of the Euler equations:

$$\frac{\partial \mathbf{U}}{\partial t}+\frac{\partial \mathbf{F}}{\partial x}+\frac{\partial \mathbf{G}}{\partial y}=0, \tag{1}$$

$$\mathbf{U}=\begin{Bmatrix}\rho\\ \rho u\\ \rho v\\ \rho E\end{Bmatrix},\quad \mathbf{F}=\begin{Bmatrix}\rho u\\ \rho u^2+p\\ \rho uv\\ \rho uH\end{Bmatrix},\quad \mathbf{G}=\begin{Bmatrix}\rho v\\ \rho uv\\ \rho v^2+p\\ \rho vH\end{Bmatrix}. \tag{2}$$

Here $\mathbf{U}$ represents the specific conservative variables per unit volume, mass, momentum and energy. $\mathbf{F}$ and $\mathbf{G}$ are the convective fluxes in the x and the y directions, in a Cartesian coordinate system, E is the stagnation specific energy and $H=E+p/\rho$ is the stagnation specific enthalpy. The numerical model is based on a Lax–Wendroff single step method (Páscoa et al., 2004). Subject to the imposed initial and boundary conditions, the solution is obtained by marching in time with

$$\mathbf{U}_{i,j}^{n+1}-\mathbf{U}_{i,j}^{n}=\Delta\mathbf{U}_{i,j}\cong-\frac{\Delta t}{\Omega_{i,j}}\left[\int_{\Omega_{i,j}}(-\mathbf{F}dy+\mathbf{G}dx)+\frac{1}{2}\int_{\Omega_{i,j}}\left(-\overline{\Delta\mathbf{F}}dy+\overline{\Delta\mathbf{G}}dx\right)\right]^{n}, \tag{3}$$

until convergence to steady state.

2.2. Camber line generator

The flow analysis algorithm performs the intensive component of the computation. A change in geometry is obtained by modifying the camber line until reaching convergence, as it is presented in Fig. 1. The distribution of mean tangential velocity, $\bar{v}$, throughout the cascade is chosen as the design variable, since it is related to the aerodynamic force on the blade section. Borges et al. (1996) have shown that the derivative of the mean tangential velocity can be expressed as:

$$-\frac{d}{dx}\left[\frac{\int_{y_{ss}}^{y_{ps}}\rho uv\,dy}{\int_{y_{ss}}^{y_{ps}}\rho u\,dy}\right]=\frac{\Delta p}{\dot{m}};\quad \bar{v}(x)=\left[\frac{\int_{y_{ss}}^{y_{ps}}\rho uv\,dy}{\int_{y_{ss}}^{y_{ps}}\rho u\,dy}\right]. \tag{4}$$

Eq. (4) shows without ambiguity that the tangential component of the force on the blade is due to the pressure difference between the suction y_{ss} and pressure y_{ps} surfaces, see Fig. 2a.

We will now present the new method of blade modification. Páscoa et al. (2004) have previously presented an inverse design formulation whose camber line generator was derived for infinitely thin blades. Albeit this the authors were able to compute thick-blade problems. With the present formulation we intended to incorporate the influence of the thickness distribution on the camber line generator. A faster convergence rate is expected to be achieved by using a more realistic model for the camber line generator.

The blade contour is defined by adding the thickness distribution $t(x)$ to the camber line $f(x)$, as can be inferred from Fig. 2b. The contour of the upper S^{+} and lower S^{-} surfaces of the blade section is given by

$$S^{+}(x)=y_0+f(x)+\frac{t(x)}{2},\quad S^{-}(x)=y_0+f(x)-\frac{t(x)}{2}. \tag{5}$$

Here y_0 refers to an arbitrary location for the leading edge of the cascade of blades with pitch s. Also, $f(x)$ is the camber line of a blade with imposed thickness $t(x)$. The slope of the streamline on the upper and lower contour lines of the blade section is given by $\frac{dS^{\pm}}{dx}=\frac{\bar{v}^{\pm}}{\bar{u}^{\pm}}$, therefore:

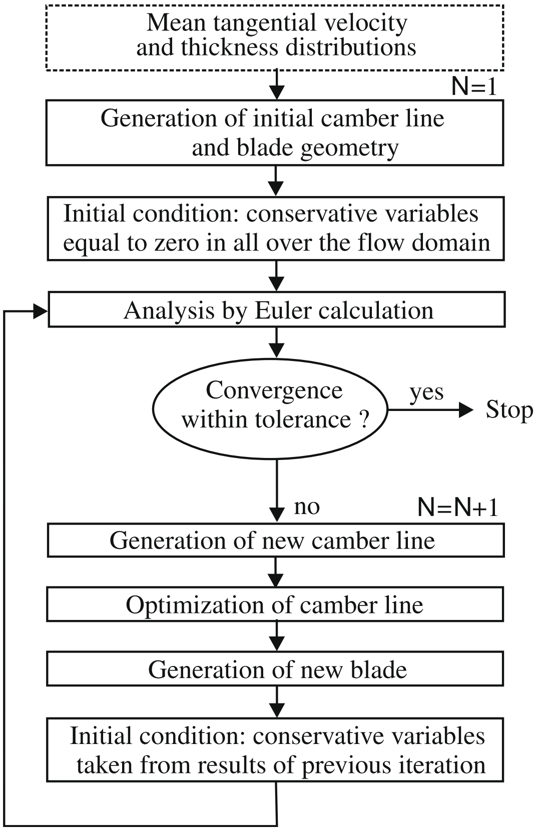

Fig. 1. Flowchart of the iterative inverse design method.

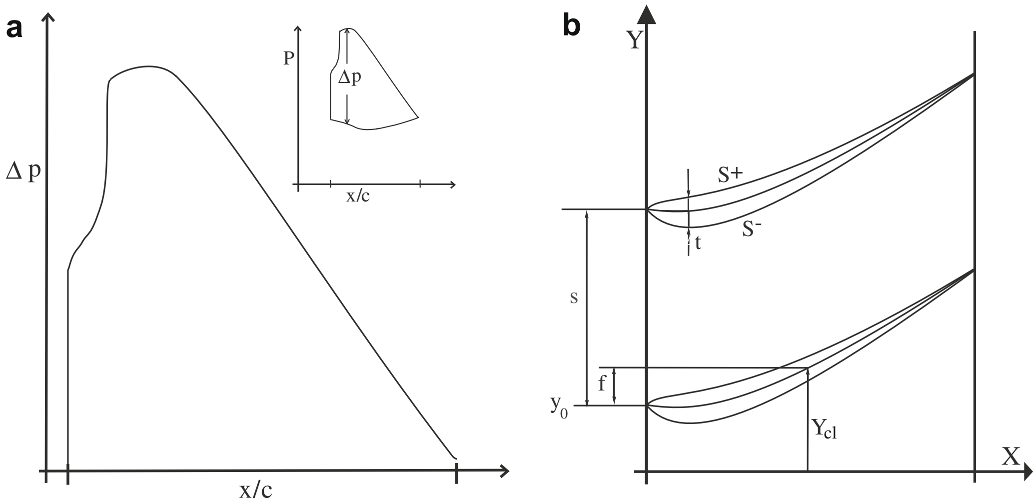

Fig. 2. (a) Definition of the load distribution as a function of Δp and (b) nomenclature for the cascade of blades.

$$\begin{cases} u^{+}\frac{\partial f}{\partial x}+\frac{u^{+}}{2}\frac{\partial t}{\partial x}=v^{+}, \\ u^{-}\frac{\partial f}{\partial x}-\frac{u^{-}}{2}\frac{\partial t}{\partial x}=v^{-}. \end{cases} \tag{6}$$

Summing up both Eq. (6) we come up with an expression that combines the slip boundary condition on both contour lines of the blade section. Applying the resulting differential equation to the design target ($*$) and to the actual (N) design iteration, we get

$$\begin{cases} \frac{df^*}{dx} = \frac{\overline{v}^*}{\overline{u}^{/*}} + \frac{1}{4}\left(\frac{\Delta u^*}{\overline{u}^{/*}}\right)\frac{dt}{dx}, \\ \frac{df^N}{dx} = \frac{\overline{v}^N}{\overline{u}^{/N}} + \frac{1}{4}\left(\frac{\Delta u^N}{\overline{u}^{/N}}\right)\frac{dt}{dx}, \end{cases} \tag{7}$$

where a linear approximation was considered for the velocity profile, between the upper and lower contours, with a mean value given by $\overline{u}^{/} = (u^+ + u^-)/2$, and the jump in axial velocity was defined as $\Delta u = (u^+ - u^-)$.

Finally, subtracting both differential equations (7), we get an ordinary differential equation that allows the computation of the new camber line approximation $(N+1)$, as a function of the kinematic variables and the blade thickness derivative. The new camber line generator is

$$\frac{df^{N+1}}{dx} = \frac{df^N}{dx} + K\left(\frac{\overline{v}^*}{\overline{u}^{/*}} - \frac{\overline{v}^N}{\overline{u}^{/N}}\right) + \frac{1}{4}\frac{dt}{dx}\left(\frac{\Delta u^N}{\overline{u}^{/N}} - \frac{\Delta u^{N-1}}{\overline{u}^{/N-1}}\right). \tag{8}$$

In Eq. (8) the jump in the axial velocity is determined with a time delay. This time-lagged formulation is introduced because this value is not known for the design conditions. For the case of infinitely thin blades, Eq. (8) results in the simpler expression given in Páscoa et al. (2004). These authors managed to design blades of finite thickness, although the physical basis of their inverse method was formulated for infinitely thin blades. It is expected that a better convergence rate can be attained by using this improved formulation:

$$\bar{u}(x) = \frac{\int_{y_s}^{y_p} \rho u dy}{\int_{y_s}^{y_p} \rho dy}; \quad \tan\beta^N = \frac{\bar{v}^N(x)}{\bar{u}_1^N}; \quad \tan\beta^* = \frac{\bar{v}^*(x)}{\bar{u}_1^*}. \tag{9}$$

As outlined in Fig. 1, we compute the mean tangential, and axial, velocity components after the first analysis of the flow through the initial cascade. The mean velocity integral in the first of Eq. (9) was used in the numerical implementation of Eq. (8) instead of the assumption of a linear velocity distribution. At the beginning of the inverse design procedure, the mean axial velocity component is only known at the entrance to the cascade and, therefore, the flow angles of the present iteration, β, and of the target iteration, β^*, are determined using the mean axial velocity at the entrance. In this approach $\bar{u}_1^N$ and $\bar{u}_1^*$ are only used to non-dimensionalize the tangential component of the velocity and, usually, they change during the design iteration procedure, until the mass flow attains the design value.

Results obtained from Eq. (8) are smoothed by means of a polynomial interpolation, in order to ensure a monotone behaviour for the camber line. The relaxation constant K is usually chosen between 0.2 and 0.6. The convergence criterion is determined by computing the maximum relative variation of camber line ordinates, $\Phi = \max\left(y_{cl}^{N+1} - y_{cl}^N\right)/y_{cl}^N$, which is usually assumed to be less than 0.1%.

The inverse method calls the flow-field analysis routine in each design iteration. The analysis code (direct) is based on an improved time-marching algorithm described in Páscoa et al. (2002). It is an explicit time-marching method that solves the Euler system of equations in 2D with a finite volume central spatial discretization. The method is enhanced with state-of-the-art artificial viscosity components based on the limiter theory. A throughout validation of the scheme was performed involving benchmark test cases.

3. Existence and uniqueness problem

Due to the lack of analytical tools for transonic flow, an empirical approach was followed to analyze the behaviour of the inverse design method.

3.1. Boundary conditions and the problem of the existence of solution

In order to overcome the problem of the existence of solution, compatibility relations must exist between the required load for the blade and the incoming flow. Since this has been analytically proved for incompressible flow it is expected the same to be true for transonic flow (Daripa, 1991).

In the context of inverse method development, the first problem is the so called consistency test. In this problem the inverse method is used to recover a blade geometry whose solution is already known. For the consistency problem the blade does originally exist, and the method should recover the blade without ambiguity. In that case there is a compatibility relation between the imposed load for the blade and the incoming flow properties. We should restate that the blade loading is explicitly imposed into the design method using the mean tangential velocity. The latter is related to the load blade shape as seen in Fig. 3a. Referring to Eq. (9), the blade load is related to the variation of the flow angle β, from upstream to downstream of the blade, and this is related to the pressure difference, Eq. (4).

However, a converged solution cannot be always reached for design tasks with an arbitrary load distribution. Then the solution is the closest geometry that satisfies both the imposed aerodynamic load and the incoming flow-field. In opposition to methods by other authors, as in Demeulenaere and van den Braembussche (1998), we note that the blade thickness is imposed as initial condition in the present method, and, therefore, a realistic blade shape (with a closed trailing edge and positive thickness) is always obtained.

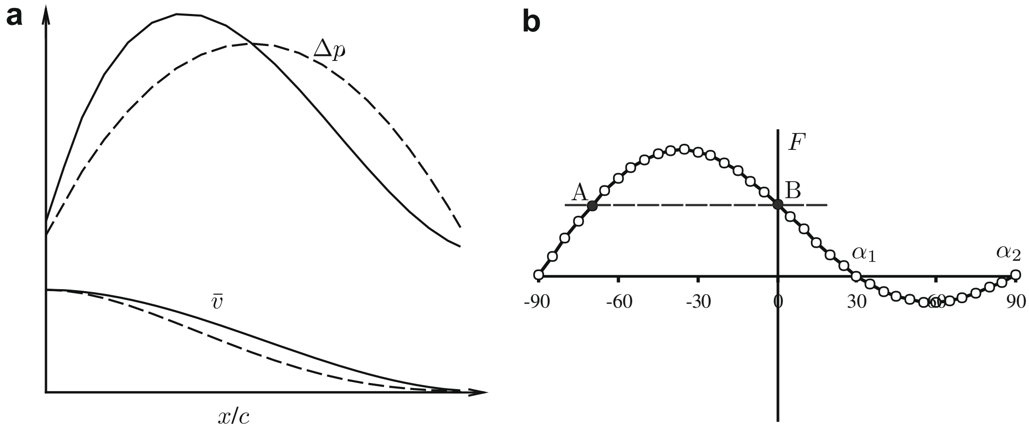

Fig. 3. (a) Imposition of blade load shape using the mean tangential velocity: symmetrical load distribution (dashed line) and a fore load distribution (solid line) and (b) theoretical computation of the load as a function of the exit flow angle α_2.

The existence problem might also be posed for the flow analysis module of the code. This is based on the solution of Euler equations with boundary conditions that are based on the characteristics theory. Consistent with the common practice for subsonic flow, we specify, at the entrance, the stagnation pressure p_{t1}, the stagnation temperature T_{t1} and the flow angle α_1, with the velocity being extrapolated from the computational domain. For subsonic exit flow the static pressure p_2 is usually imposed, and the three remaining primitive variables are extrapolated from inside the computational domain. This will ensure that the analysis code is properly formulated regarding the boundary conditions (Ferlauto et al., 2004).

3.2. Analysis of solution uniqueness

For steady flow, the tangential force acting on a blade can be related to the tangential component of the velocity upstream and downstream of the cascade of blades, $F = \dot{m}(v_1 - v_2)$. As referred by Zannetti and Pandolfi (1984), F changes as a function of exit flow angle α_2, see Fig. 3b. Starting from a set of values for p_{t1}, T_{t1}, α_1 and p_2 we determine $F(\alpha_2)$ for a general cascade. The data plotted in Fig. 3b was obtained analytically from the homentropic flow relations. It is clearly seen that F will be zero for three values of α_2. For $\alpha_2 = \pm 90^\circ$, u_2 and, as a consequence, $\dot{m}$ vanish. Besides, F also vanishes for $\alpha_2 = \alpha_1$, that is, when the blade does not deflect the flow. The force is positive for $\alpha_2 < \alpha_1$.

Now we consider the inverse problem that must be solved by imposing a set of boundary conditions (p_{t1}, T_{t1}, α_1 and p_2) and a load distribution $\Delta p(x)$, or mean tangential velocity $\bar{v}(x)$. Taking into account the previous considerations, in general there will be two possible blade geometries that meet the required conditions, or any other.

The tangential force can be determined from $F = \int \Delta p(x)dx$, with the integral taken along the x-axis between the leading and trailing edges of the blade. For $F > F_{max}$ or $F < F_{min}$ there will be no solution, but for $F_{min} < F < F_{max}$ there will be two cascades of blades that can provide the same tangential force (as seen from points A and B in Fig. 3b). Therefore, the same tangential force can be obtained by a lower mass flow-rate and a larger flow deflection, as in case A, or by a higher mass flow-rate and smaller flow deflection, as in case B.

4. Numerical results

This section presents the efficiency gains obtained with the new formulation for the camber line generator. A check on the existence and uniqueness problem, using the empirical approach, is also presented.

4.1. The efficiency of the novel formulation

A consistency test was made to evaluate the performance of the new formulation for the camber line generator. This consisted in using the design code to redesign an already known geometry. This precluded any existence and uniqueness problems by concentrating our check only on the camber line generator.

Fig. 4a presents the changes in geometry for the initial, target and original blade section. Less than 1% difference was obtained between the target and final designed mean camberline geometry. The changes in the flow-field are shown in Fig. 7. The mean tangential velocity is the imposed design variable, Fig. 4b. Good agreement for the original and target values was obtained, with minor discrepancies on suction surface sonic bubbles. This is mainly due to a weakness of the analysis module of the code near sonic areas, a typical behaviour of some time-marching algorithms.

The numerical efficiency of the method can be seen from the analysis of the convergence rate. Fig. 5a presents the evolution of the inverse method convergence criterion as a function of the design iterations. Results plotted in Fig. 5b show a

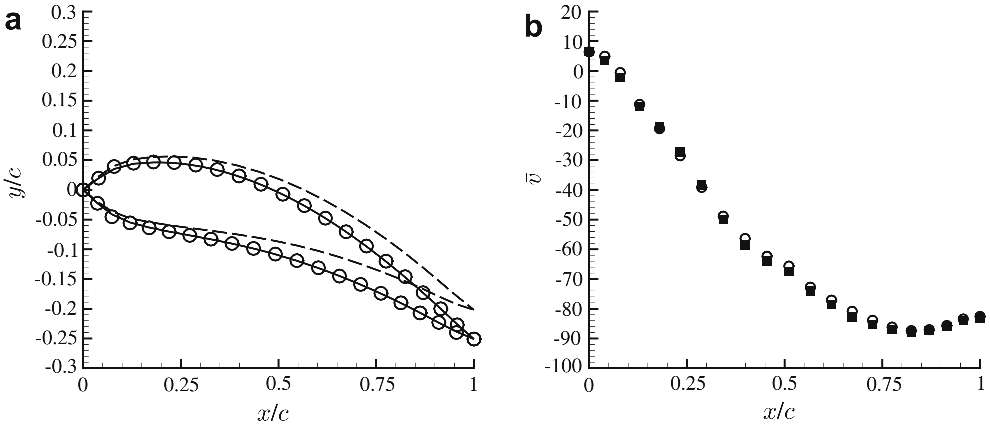

Fig. 4. (a) Geometry of the target (line), initial (dashed) and final designed blade (circles) and (b) evolution of the mean tangential velocity for the target (black squares) and the final designed blade (circles).

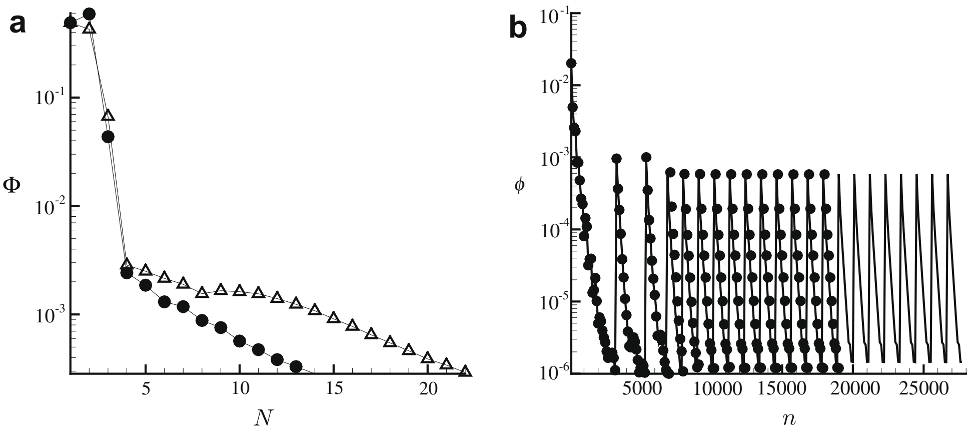

Fig. 5. (a) Convergence of the design criterion as a function of the design iterations and (b) convergence of the flow-field analysis code for the several design iterations. Here symbol '△' refers to results using the earlier formulation of Páscoa et al. (2004) and symbol '•' denotes the results of the present formulation.

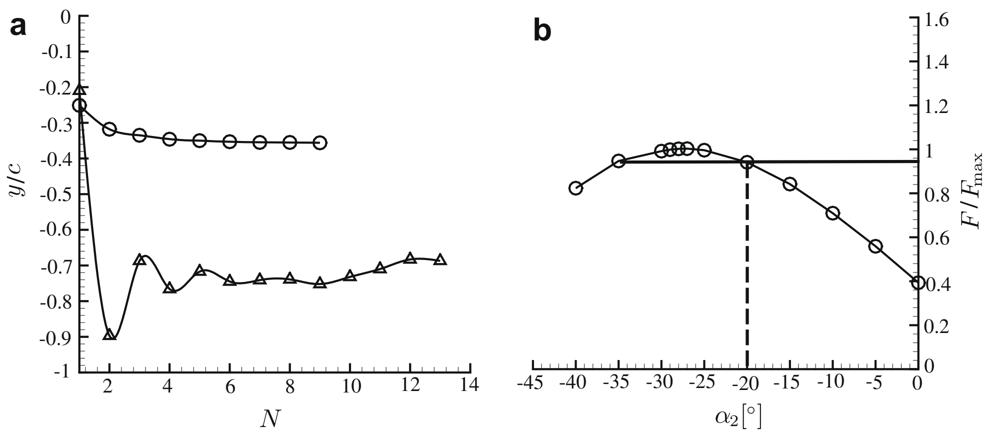

Fig. 6. (a) Evolution of trailing edge position during the inverse design procedure. Results for two exit flow angles, $\alpha_2 = -20^\circ$ (○ symbol) and $\alpha_2 = -35^\circ$ (△ symbol). (b) Experimental computation of the load as a function of the exit flow angle α_2 ($^\circ$). The discrete symbol '○' refers to results from the finite volume analysis code.

more evident gain on the overall design time for the inverse design procedure. This is evident by looking at the convergence rate of the analysis code.

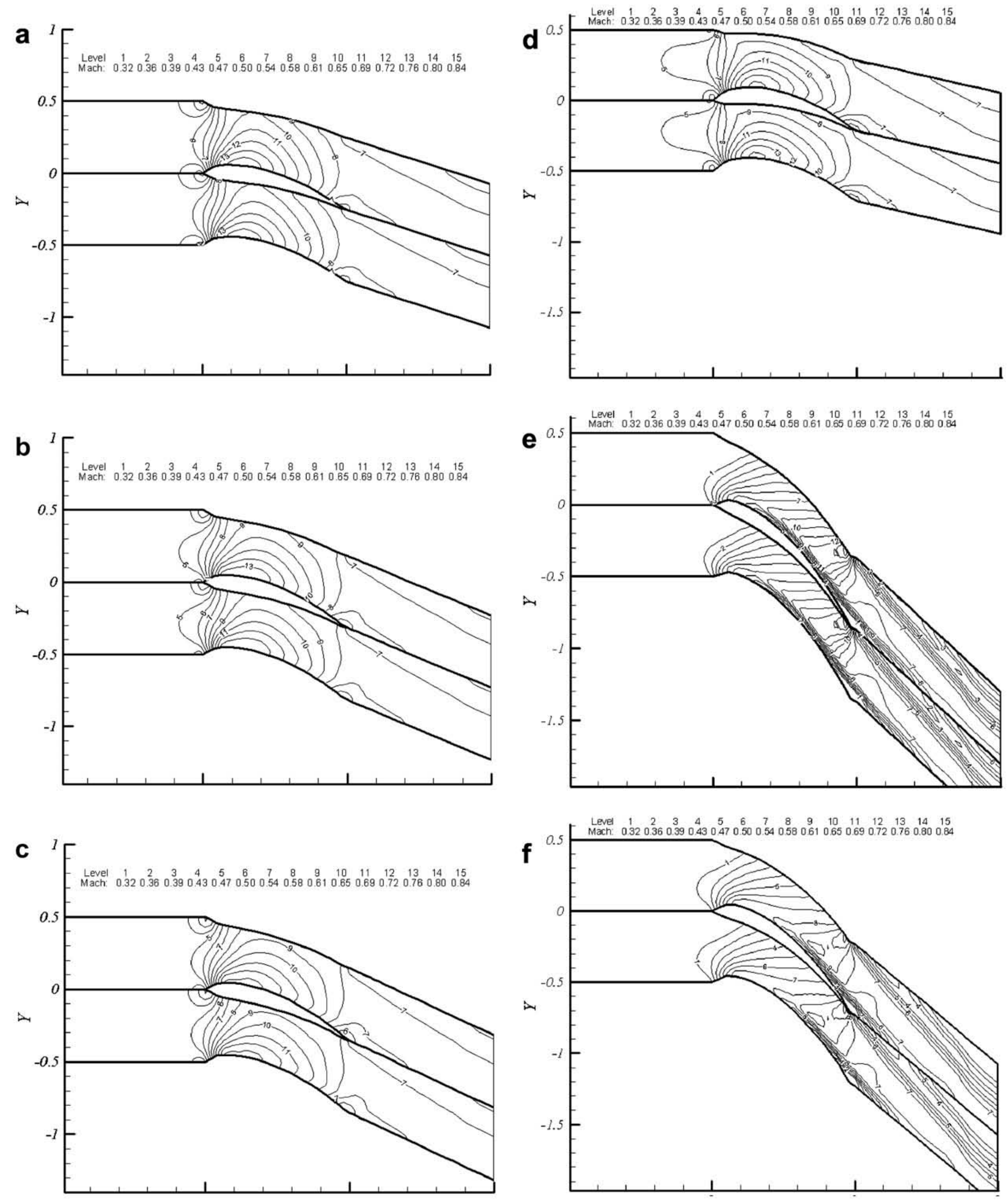

Fig. 7. Evolution of the flow-field during the design iterations: (a) first design iteration for $\alpha_2 = -20^\circ$; (b) second design iteration for $\alpha_2 = -20^\circ$; (c) last design iteration for $\alpha_2 = -20^\circ$; (d) first design iteration for $\alpha_2 = -35^\circ$; (e) second design iteration for $\alpha_2 = -35^\circ$; and (f) last design iteration for $\alpha_2 = -35^\circ$.

4.2. Empirical assessment of the existence and uniqueness problems

In order to check for the behaviour illustrated in Fig. 3b the present inverse method was used to redesign a cascade consisting of NACA0012 blades. The imposed pitch–chord ratio is 0.5. The conditions specified for the inflow are Ma_1 = 0.55 and

$\alpha_1 = 5^\circ$. Fig. 6b shows the evolution of the blade section tangential force obtained through multiple analysis of the flow though the cascade, for different exit flow angles α_2. The evolution of the graph is quite similar to that presented in Fig. 3b. Results plotted in Fig. 6b for this cascade show that the same tangential force is obtained for $\alpha_2 = -20^\circ$ and $\alpha_2 = -35^\circ$. We observe that the mass flow for $\alpha_2 = -35^\circ$ is 79% lower than the one obtained for $\alpha_2 = -20^\circ$. This behaviour could be prone to uniqueness problems, as referred by other authors using different formulations for the inverse method (Demeulenaere and van den Braembussche, 1998).

Results from the analysis presented in Fig. 6b were given as input to run the code, in design mode, to redesign the two cascades of blades defined for an exit flow angle of $\alpha_2 = -35^\circ$ and $\alpha_2 = -20^\circ$. Both blade sections were recovered under the same convergence criterion $\Phi \leq 1\%$ (Páscoa, 2007).

The evolution of the position of the trailing edge throughout the design process is plotted in Fig. 6a. It is clear that for $\alpha_2 = -20^\circ$ the cascade of blades shows a monotone evolution for the position of the trailing edge, and it reaches convergence after nine design iterations. For the cascade with $\alpha_2 = -35^\circ$ the behaviour of the trailing edge position is quite oscillatory, as seen from Fig. 6a. Fig. 7 shows the evolution of the cascade geometry, and flow-field, during the inverse design. For the most severe case, for $\alpha_2 = -35^\circ$, the method was able to recover the blade at the expense of an increase in design time. For a mesh composed of 4000 nodes, and using the new formulation, the typical design time is 3 h on a Pentium processor at 2 GHz.

5. Conclusions

This work describes a new formulation for an iterative inverse design method that is able to design turbomachinery cascades of blades. The formulation incorporates a thickness distribution term that introduces a more realistic model for the camber line generator. An increase in the convergence rate of the method was obtained with the new formulation.

The theory behind the design method was further investigated by analyzing the problem of the existence and uniqueness of solution. Analytical solutions for the problem of existence and uniqueness of solution are not available for rotational transonic compressible flow. We tackled the problem using an empirical approach to assess the existence and uniqueness problem.

It became clear during the study that the present inverse method is always able to come up with a realistic blade section geometry and can provide a solution, at least approximate, for the case were there is no compatibility between the incoming flow properties and the prescribed load. Typically, and in the context of the present method, we conclude that for low stagger angles the method converges monotonically to the target cascade geometry. For high stagger angles, particularly for those larger than that corresponding to the maximum blade section tangential force, the method shows an oscillatory behaviour during convergence to the target cascade. The same non-monotone convergence behaviour was observed when performing the same analysis for different cascades, under different flow conditions. Albeit this, the proposed formulation does actually converge to the target blade geometry, but presents lower convergence rate under these conditions.

Acknowledgements

This work was partly funded by Fundação para a Ciência e Tecnologia in the framework of Project PTDC/EME-MFE/66608/2006, *Intelligent Inverse Design Method for LP-Turbine Rows in Viscous Flow*. The support of Prof. J.E.T. Borges in the earlier stages of the work is gratefully acknowledged.

References

Borges, J.E.T., Gato, L.M.C., Pereira, R.M.R.J., 1996. Iterative use of a time-marching code for designing turbomachine blade rows. Computers & Fluids 25 (2), 197–216.

Daripa, P., 1991. Solvability condition and its application to fast numerical solution of overposed inverse problems in compressible flows. Journal of Computational Physics 95, 436–449.

Demeulenaere, A., van den Braembussche, R.A., 1998. Three-dimensional inverse method for turbomachinery blading design. Journal of Turbomachinery 120, 247–255.

Ferlauto, M., Iollo, A., Zannetti, L., 2004. Set of boundary conditions for aerodynamic design. AIAA Journal 42 (8), 1582–1592.

Hawthorne, W.R., Wang, C., Tan, C.S., McCune, J.E., 1984. Theory of blade design for large deflections: part I – two-dimensional cascade. ASME Journal of Engineering for Gas Turbines and Power 106, 346–353.

Lee, J.W., Mason, W.H., 2000. Inverse solution uniqueness and domain of existence for space-marching applications. AIAA Journal 38 (1), 44–49.

Lighthill, J., 1945. A New Method of Two-dimensional Aerodynamic Design. Tech. Report, Aeronautical Research Council, R&M 2112.

Páscoa, J.C., 2007. Development of 3D Methodologies for Analysis and Inverse Design of Turbomachinery Cascades of Blades in Compressible Flow (in Portuguese). Ph.D. thesis, Universidade da Beira Interior, Portugal.

Páscoa, J.C., Mendes, A.C., Gato, L.M.C., 2002. An efficient finite volume scheme with improved artificial viscosity suitable for transonic-flow calculations. International Series on Advances in Fluid Mechanics, vol. 32. WIT Press, pp. 505–514.

Páscoa, J.C., Mendes, A.C., Gato, L.M.C., Elder, R., 2004. Aerodynamic design of turbomachinery cascades using an enhanced time-marching finite volume method. CMES – Computer Modeling in Engineering & Sciences 6 (6), 537–546.

Volpe, G., Melnik, R.E., 1981. Role of constraints in inverse design for transonic airfoils. AIAA Journal 22 (12), 1770–1778.

Zannetti, L., Pandolfi, M., 1984. Inverse Design Technique for Cascades. Tech. Report, NASA-CR-3836.